Superresolved phase-shifting Gabor holography by CCD shift

2009 J. Opt. A: Pure Appl. Opt. 11 125408

(http://iopscience.iop.org/1464-4258/11/12/125408)

J. Opt. A: Pure Appl. Opt. **11** (2009) 125408 (6pp) doi:10.1088/1464-4258/11/12/125408

Superresolved phase-shifting Gabor holography by CCD shift

V Micó[1], L Granero[2], Z Zalevsky[3] and J García[1]

[1] Departamento de Óptica, Universitat de València, C/Dr Moliner, 50, 46100 Burjassot, Spain
[2] AIDO—Technological Institute of Optics, Color and Imaging, C/Nicolás Copérnico 7-13, 46980 Paterna, Spain
[3] School of Engineering, Bar-Ilan University, Ramat-Gan, 52900, Israel

E-mail: Vicente.Mico@uv.es

Received 4 July 2009, accepted for publication 11 August 2009
Published 21 September 2009
Online at stacks.iop.org/JOptA/11/125408

Abstract
Holography in the Gabor regime is restricted to weak diffraction assumptions. Otherwise, diffraction prevents an accurate recovery of the object's complex wavefront. We have recently proposed a modified Gabor-like setup to extend Gabor's concept to any sample provided that it be non-diffusive. However, the resolution of the final image becomes limited as a consequence of the additional elements considered in the proposed setup. In this paper we present an experimental approach to overcome such a limitation in which the former configuration is used while the CCD camera is shifted to different off-axis positions in order to generate a synthetic aperture. Thus, once the whole image set is recorded and digitally processed for each camera position, we merge the resulting band-pass images into one image by assembling a synthetic aperture. Finally, a superresolved image is recovered by Fourier transformation of the information contained in the generated synthetic aperture. Experimental results validate our concepts for a gain in resolution of close to 2.

Keywords: digital holography, synthetic aperture generation, Fourier image formation, and superresolution

(Some figures in this article are in colour only in the electronic version)

1. Introduction

In-line microscopy without lenses (or lensless microscopy) was originally proposed by Gabor as a method to overcome the limitations introduced by lenses in electron microscopy [1]. Basically, Gabor's concept is based on an in-line architecture, where the sample is illuminated by a coherent beam and a recording device, which is placed behind the sample, records the produced diffracted wavefront which is known as Gabor's hologram. In this configuration, the non-diffracted light plays the role of a reference beam that interferes with the diffracted components generated by the sample. Thus, it is possible to recover the object's complex wavefront by using classical holographic tools in the reconstruction process. However, Gabor's concept needs to be applied under severe sample constraints: the samples must be considered as weak diffractive. Only in this case, can the sample's diffracted light be considered as a perturbation of the reference beam and Gabor's underlying principle become true. Otherwise, the amount of light blocked by the object is significant and the diffraction which dominates the process will prevent the sample's complex wavefront from being accurately recovered.

The simplest way to remove the Gabor limitation is by reinserting a reference beam at the recording plane. Thus, holography dominates the process independently of the type of imaged object. Leith and Upatnieks [2–4] reported on different off-line holographic schemes that improve the final image reconstruction since they avoid the distortion caused by overlapping, in the observation direction, of the three holographic terms arising from the in-line architecture.

Nowadays, digital lensless in-line holographic microscopy (the original idea proposed by Gabor merged nowadays with digital capabilities) combines the development of modern solid-state image sensors with the numerical processing capabilities that are provided by computers. This type of holography has a variety of applications in three-dimensional

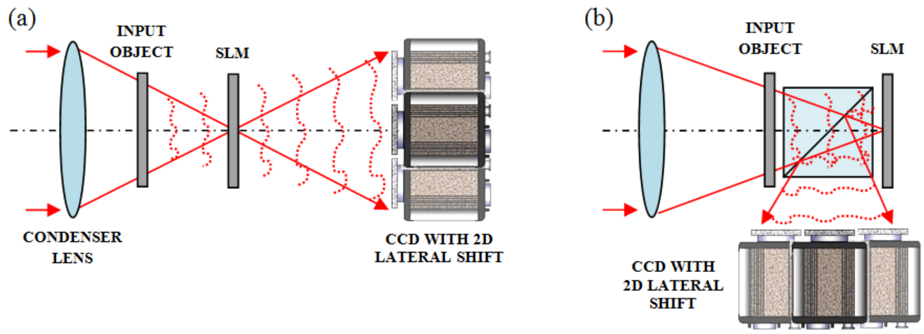

Figure 1. Experimental setup arrangement for the proposed approach: (a) transmissive and (b) reflective configurations.

(3D) imaging with micrometer resolution including underwater observations, tracking moving objects and particles, as well as the study of erosion processes in coastal sediments [5–14]. However, all of these approaches suffer from the same limitation reported in the original idea of Gabor. Once again, and in the same direction pointed out by Leith and Upatnieks, digital in-line holography applying an external reference beam has also been reported on extensively in the literature [15, 16]. Other ingenious approaches are based on digital lensless Fourier holographic architectures where the object and the reference beams are generated from the same plane, following a common path until reaching the CCD [17, 18].

Recently, Micó *et al* have validated a new concept in the field of Gabor's holography that allows the recovery of the complex amplitude of the wavefront incoming from the sample [19]. It is based on a Gabor-like setup, but with the addition of two new elements. First, a condenser lens, between the input sample and the CCD, which provides focusing of the illumination at an intermediate plane (Fourier plane). And second, a spatial light modulator (SLM) which is placed at the Fourier plane to allow a phase-shifting procedure [20, 21] by modulating its pixels according to the DC term of the object spectrum. With these modifications, the approach reported in [19] becomes useful for any kind of sample (not only weakly diffracting objects as in Gabor's concept), it removes both zero order and twin image terms from the reconstruction (avoiding distortion and improving the signal-to-noise ratio in the reconstructed images), and eliminates the need to perform coordinate transformation for high numerical apertures and magnifications (because the complex amplitude distribution can be precisely propagated). However, due to the need to locate the Fourier plane between the sample and CCD, the achievable resolution of the method is reduced by diffraction [22], since it is related to the distance between the sample and the CCD (among other factors).

In this paper, we present a combination of techniques that enable one to overcome the resolution limit imposed by diffraction in the configuration presented in [19]. The basic principle is based on shifting the CCD to different off-axis positions in order to synthesize an expanded aperture which improves the system's resolution. Although other authors had also implemented synthetic aperture methods by shifting the CCD [23–28], the presented application is novel and provides highly promising results. Essentially, the way to recover each frequency band corresponding to each CCD position is the same one as described in [19]. Since the central part of the sample's spectrum is responsible for the DC term of the image, that is, for the non-diffracted light in Gabor's concept, the recorded in-line hologram can be phase shifted in time by modulating that pixel of the SLM which spatially coincides with the DC term. By previous calibration of the phase-step produced by the SLM, the complex amplitude distribution of the diffracted sample wavefront can be recovered by applying conventional phase-shifting algorithms. This procedure is applied to each one of the recording positions of the CCD camera. Following that, the recovered distribution can be propagated digitally up to the object plane by taking into account a linear phase factor in the back propagation. Such a linear phase factor comes from the CCD displacement. Finally, all the propagated distributions are used to assemble a synthetic expanded aperture that yields a superresolved image by Fourier transformation.

Thus, and in summary, the whole proposed procedure could be understood as a technique based on time multiplexing the spatial-frequency content diffracted by the input sample in a similar way to that which sequential off-axis illumination performs in digital holographic microscopy [29–36], but where the synthetic aperture is generated by CCD displacement [23–28]. The way to recover the complex wavefront diffracted by the object is by phase-shifting the DC term of the object spectrum in a similar way to that performed in common-path point-diffraction interferometers [37–41]. This mixing of methods is first described in section 2 and experimentally validated in section 3.

2. System description and methodology

The experimental setup is depicted in figure 1 and can be implemented in both transmissive and reflective configurations. As can be seen, a condenser lens is used to focus the laser beam onto the SLM and the input object is placed between the lens and the SLM. In this configuration, the object spectrum is generated at the SLM plane. Finally, a CCD camera records the incoming amplitude distribution. For the reflective configuration, a beam splitter is needed to allow the recording process.

Considering this architecture, it is possible to recover the complex amplitude distribution of the wavefront that is diffracted by the input object [19]. Basically, the technique implies the modulation of the DC term of the image (central part of the object spectrum) by phase modulating the pixels of the SLM that coincide with the spatial position of the DC term. Thus, after preliminary calibration of the phase-step introduced by the SLM, it is possible to apply a conventional phase-shifting procedure over the intensity images that are provided by the CCD [16]. In the experiments, the SLM provides 64 phase levels covering the required full 2π range. Since the pixel size of the SLM is smaller than the central lobe of the spectrum (given by the object extent and its distance to the CCD [41]), an accurate and controllable phase reconstruction is expected. Thus, an in-line hologram is recorded by the CCD and stored in the computer's memory for each of the 64 phases originated at the SLM. After that, a phase-shifting algorithm is applied to the whole set of 64 stored intensities to perform the recovery of the complex wavefront that is diffracted by the input object. And finally, the resulting amplitude distribution is digitally back propagated to the object plane using the convolution method applied to the diffraction Rayleigh–Sommerfeld integral [17, 19]. This method can be applied provided that there is a DC term in the object spectrum and without the need for the weak diffraction assumption (as required for conventional Gabor holograms).

Now, we will focus on the way to improve the resolution of the method reported in [19]. Since the method needs to provide the object spectrum in a plane between the input object and the CCD camera, there is a minimum distance at which to locate the CCD after the input object. Given the CCD sensor size, such a distance is related to the numerical aperture (NA) of the condenser lens in the transmissive configuration, and with the condenser lens NA and the size of the beam splitter in the reflective configuration. Let us call this distance d. This fact means that the resolution of the proposed imaging system will be limited according to the relation $R_i = \lambda/\mathrm{NA}_i$, where R is the resolution of the imaging system, λ is the illumination wavelength, NA is the numerical aperture defined by the CCD size at distance d from the input object, and the sub-index i designates the horizontal and vertical directions (given that the CCD is rectangular). So, different resolution limits, that depend on the selected observation direction, are obtained.

To overcome this resolution limit, we propose shifting the CCD in order to generate a synthetic aperture. Since the object that was selected to validate the proposed method is composed of horizontal and vertical lines, we shift the CCD to 4 off-axis positions (2 horizontally and 2 vertically), but any other synthetic aperture could be synthesized if it is required. The only restriction to apply in the proposed method is that the NA of the condenser lens should be high enough to ensure non-diffracted light (reference beam) at the positions where the CCD is displaced. This situation is depicted in figure 1. Thus, the synthetic numerical aperture (SNA) can be expanded until reaching at least the NA of the condenser lens. However, since the CCD is a few millimeters in size, the NA of the condenser lens is not a restrictive factor.

Once the phase-shifting procedure is applied for a given CCD off-axis recording position, we perform back propagation up to the input plane, by taking into account a linear phase factor in the propagation, to allow the overlapping of the same portion of the object field of view. This linear phase is responsible for a prismatic effect in the propagation and it can be calculated, first by visual criterion, and then a fine adjustment is obtained by maximizing the correlation peak between the on-axis recovered image and the off-axis ones when considering different linear phases. Thus, we ensure the recovery of a different spectral content of the same input object field of view.

Finally, a synthetic aperture is assembled by placing the spatial-frequency content of the recovered band-pass images to its original position in the object spectrum. However, a fine adjustment of the phase of each band-pass image is needed, since each recording position will have different recording phase conditions due mainly to two reasons. First, we must consider the addition of a global phase to each recovered band-pass image. This global phase is due to subwavelength distance mismatches in the optical path that are impossible to match on each recording separately. And second, we find the replacement of each recovered rectangular aperture to its original position in the object spectrum. This procedure is achieved in two steps. By knowing the displacement of the CCD in comparison to the CCD size, it is possible to add a linear phase factor to the recovered band-pass image in order to shift each elementary aperture to its rough position in the Fourier domain. Later, a final and fine adjustment is achieved by the addition of smaller linear phase factors in both horizontal and vertical directions. In addition, this fine tuning process compensates for phase variations coming from misalignments in the optical setup. This procedure is repeated for every elementary rectangular aperture considered in the experiment. The full adjustment can be guided by an image quality criterion and automated to yield a superresolved image by simple inverse Fourier transformation of the information contained in the generated synthetic aperture.

3. Experimental validation

The reflective configuration that is depicted in figure 1 was selected for the experimental implementation, and it is presented in figure 2. A doublet lens (80 mm focal length and 60 mm diameter) is used as a condenser lens to focus the laser beam (532 nm wavelength) onto a reflective SLM (Holoeye HEO 1080 P, 1920 pixel × 1080 pixel resolution, 8 μm pixel pitch). The SLM is controlled by a computer that allows the gray levels to be changed for the relevant pixels of SLM that coincide with the DC term of the object spectrum. A negative USAF resolution test target is used as an input object to demonstrate the resolution improvement. Finally, a beam splitter cube (20 mm × 20 mm size) is used to reflect the light onto a CCD camera (Basler A312f, 582 pixels × 782 pixels, 8.3 μm pixel size, 12 bits/pixel). Optical mounts and micrometric translation stages complete the experimental setup.

As an example of back propagation with different linear phase factors, figure 3 shows the case when the CCD is shifted to a left (horizontal) position. From case (a), corresponding

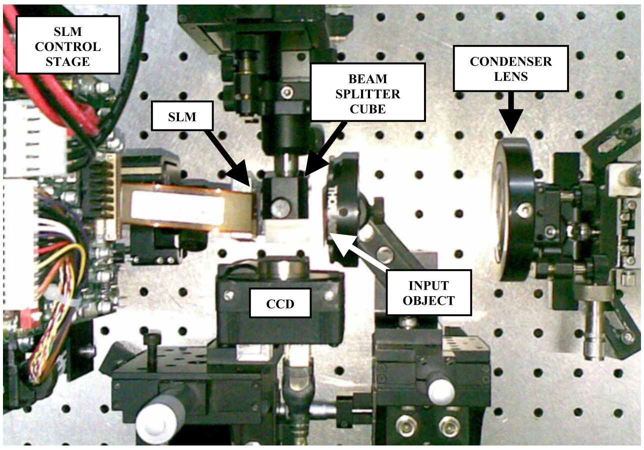

Figure 2. Experimental setup assembled at the laboratory in a reflective configuration.

with a zero factor, to case (d) we can see as the input object field of view is shifted according to the introduced linear phase. By fine adjustment of the added linear phase factor, it is possible to properly overlap the region of interest of the object field of view.

Figure 4 shows the recovered band-pass images corresponding with (a) on-axis, (b) one vertical and (c) one horizontal off-axis recording positions of the CCD. We can see how the high order spatial-frequency content, which comes from outside the limited rectangular CCD aperture, is now accessible from those images. Case (a) corresponds to the low resolution image provided by the conventional imaging system that is used in the reported work.

When the four off-axis band-pass images alongside the on-axis one are numerically processed, they are used to assemble the synthetic aperture which is depicted in figure 5. This is done in comparison with the conventional rectangular aperture obtained when only the on-axis CCD position is considered. We have studied the case when a resolution gain factor of 2 is pursued in both horizontal and vertical directions. This fact means that the CCD is shifted 3.25 and 2.42 mm in horizontal and vertical directions, respectively, according to the CCD dimensions and the pixel size. As the distance between the input object and the CCD is approximately 75 mm, the NA's in the horizontal and vertical directions for the conventional imaging system are 0.043 and 0.032, respectively, and the theoretical expected SNA's after applying the proposed approach are 0.086 and 0.064, respectively.

Finally, figure 6 presents the conventional (a) and superresolved (b) images obtained without and with applying the proposed method. Several insets in both images enhance the resolution limits for clarity. In the conventional imaging mode and according with theory, the theoretical resolution limits in the horizontal and vertical directions are $R_H = 12.4\ \mu$m (80.6 lp mm^{-1}) and $R_V = 16.6\ \mu$m (60.2 lp mm^{-1}). In figure 6(a) we can see the resolution limits are Group6-Element2 (71.8 lp mm^{-1}) and Group5-Element5 (50.8 lp mm^{-1}); in good agreement with the theoretical values R_H and R_V. When the superresolution method is applied, the resolution limits improve to Group7-Element2 (144 lp mm^{-1} or 6.9 μm) and Group6-Element6 (114 lp mm^{-1} or 8.8 μm), which means a resolution gain factor of 1.8 and 1.9 in the horizontal and vertical directions respectively, and an SNA of 0.077 and 0.06 in the horizontal and vertical directions, respectively. As we can see, both the gain in resolution and the SNA values are close to the expected ones.

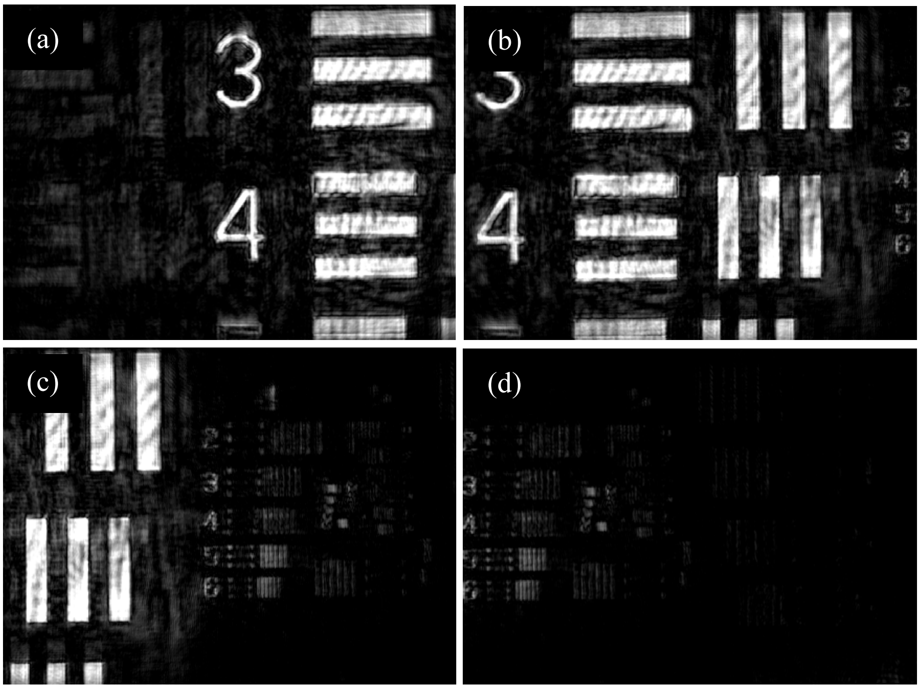

Figure 3. Back propagation to the input plane of the recovered complex wavefront that corresponds to a horizontal off-axis CCD position. The back propagation is done while considering the different linear phases.

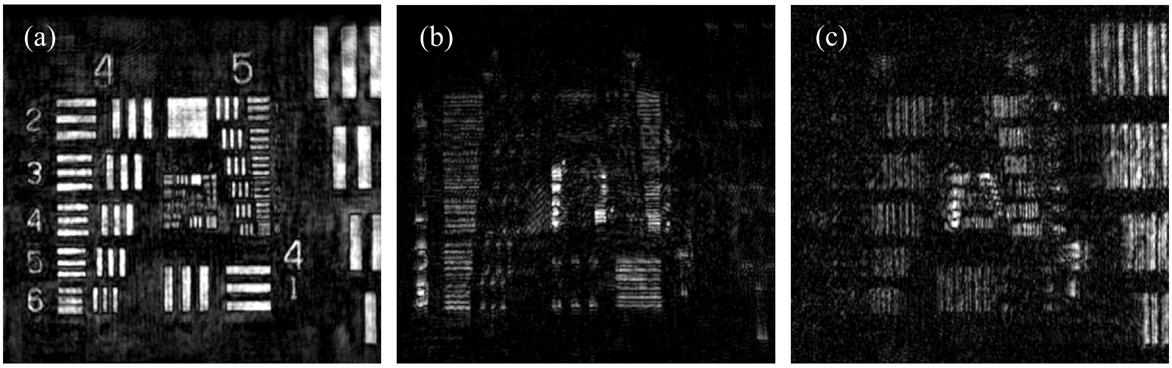

Figure 4. Recovered band-pass images corresponding to (a) on-axis CCD position, and (b) vertical and (c) horizontal displacements of the CCD. The introduced linear phase factors for cases (b) and (c) imply carrier frequencies of 60.7 mm^{-1} and 81.3 mm^{-1}, respectively, or, in other words, deviation angles of 1.85° and 2.48°, respectively.

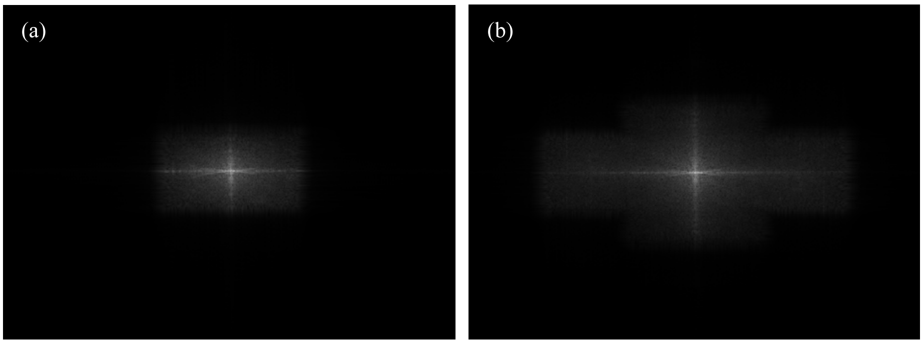

Figure 5. (a) Conventional aperture of the imaging system and (b) generated synthetic aperture considering the proposed approach.

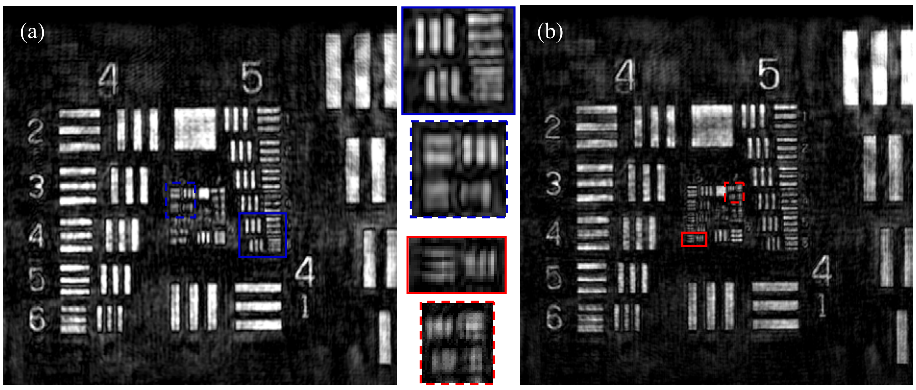

Figure 6. (a) The conventional image corresponding to the on-axis CCD position and (b) the superresolved image that is obtained when applying the proposed approach. The inner row of images enhances the resolution limits in the horizontal (dashed) and vertical (solid) directions for the conventional (first two images from top to bottom with blue frame) and superresolved (last two images from top to bottom with red case) images in order to clearly show the superresolution effect.

4. Conclusions

We have experimentally demonstrated a method that is useful to improve the limited resolution of the setup recently reported in [19]. It is based on the generation of a synthetic aperture by shifting the CCD camera to a set of off-axis positions and then the recovery, for each position, of the complex wavefront incoming from the region of interest of an object illuminated with laser light. The procedure to recover the complex amplitude distribution is based on the proof of the principles proposed in [19] but now has the addition of a linear phase in the digital back propagation towards the input plane for the off-axis CCD positions. Once the input object is digitally refocused, all the different spatial-frequency content incoming from the set of off-axis positions is merged into one by assembling a synthetic aperture. Finally, a superresolved image is obtained as the simple Fourier transformation of the information contained in the synthetic aperture. Experimental results validate our theoretical predictions.

Additional advantages come from the inherent holographic nature of the process. Since the proposed method recovers both the amplitude and phase information that is diffracted by the object, quantitative superresolved phase information (in a way that is similar to the approach discussed in [35]), and superresolved imaging for 3D samples (in a way that is similar to [36]) are also possible.

Acknowledgment

This work has been partially supported by the Spanish Ministerio de Educación y Ciencia under the project FIS2007-60626.

References

[1] Gabor D 1948 A new microscopic principle *Nature* **161** 777–8
[2] Leith E N and Upatnieks J 1962 Reconstructed wavefronts and communication theory *J. Opt. Soc. Am.* **52** 1123–30
[3] Leith E N and Upatnieks J 1963 Wavefront reconstruction with continous-tone objects *J. Opt. Soc. Am.* **53** 1377–81
[4] Leith E N and Upatnieks J 1964 Wavefront reconstruction with diffuse illumination and three-dimensional objects *J. Opt. Soc. Am.* **54** 1295–301
[5] Xu W, Jericho M H, Meinertzhagen I A and Kreuzer H J 2001 Digital in-line holography for biological applications *Proc. Natl Acad. Sci. USA* **98** 11301–5
[6] Watson J *et al* 2001 Simultaneous in-line and off-axis subsea holographic recording of plankton and other marine particles *Meas. Sci. Technol.* **12** L9–15
[7] Hobson P R and Watson J 2002 The principles and practice of holographic recording of plankton *J. Opt. A: Pure Appl. Opt.* **4** S34–49
[8] Pedrini G and Tiziani H J 2002 Short-coherence digital microscopy by use of a lensless holographic imaging system *Appl. Opt.* **41** 4489–96
[9] Xu W, Jericho M H, Meinertzhagen I A and Kreuzer H J 2003 Tracking particles in 4D with in-line holographic microscopy *Opt. Lett.* **28** 164–6
[10] Sun H, Perkins R G, Watson J, Player M A and Paterson D M 2004 Observations of coastal sediment erosion using in-line holography *J. Opt. A: Pure Appl. Opt.* **6** 703–10
[11] Malkiel E, Abras J N and Katz J 2004 Automated scanning and measurements of particle distributions within a holographic reconstructed volume *Meas. Sci. Technol.* **15** 601–12
[12] Repetto L, Piano E and Pontiggia C 2004 Lensless digital holographic microscope with light-emitting diode illumination *Opt. Lett.* **29** 1132–4
[13] Garcia-Sucerquia J, Xu W, Jericho S K, Klages P, Jericho M H and Kreuzer H J 2006 Digital in-line holographic microscopy *Appl. Opt.* **45** 836–50
[14] Garcia-Sucerquia J, Xu W, Jericho M H and Kreuzer H J 2006 Immersion digital in-line holographic microscopy *Opt. Lett.* **31** 1211–3
[15] Schnars U and Jueptner W P 2005 *Digital Holography* (Berlin: Springer)
[16] Kreis T 2005 *Handbook of Holographic Interferometry: Optical and Digital Methods* (Weinheim: Wiley–VCH Verlag GmbH & Co. KGaA)
[17] Haddad W S, Cullen D, Solem J C, Longworth J W, McPherson A, Boyer K and Rhodes Ch K 1992 Fourier-transform holographic microscope *Appl. Opt.* **31** 4973–8
[18] Takaki Y and Ohzu H 1999 Fast numerical reconstruction technique for high-resolution hybrid holographic microscopy *Appl. Opt.* **38** 2204–11
[19] Micó V, García J, Zalevsky Z and Javidi B 2009 Phase-shifting Gabor holography *Opt. Lett.* **34** 1492–4
[20] Yamaguchi I and Zhang T 1997 Phase-shifting digital holography *Opt. Lett.* **22** 1268–70
[21] Yamaguchi I, Kato J, Ohta S and Mizuno J 2001 Image formation in phase-shifting digital holography and applications to microscopy *Appl. Opt.* **40** 6177–85
[22] Abbe E 1873 Beitrage zur theorie des mikroskops und der mikroskopischen wahrnehmung *Arch. Mikrosk. Anat.* **9** 413–68
[23] Le Clerc F, Gross M and Collot L 2001 Synthetic aperture experiment in the visible with on-axis digital heterodyne holography *Opt. Lett.* **26** 1550–2
[24] Massig J H 2002 Digital off-axis holography with a synthetic aperture *Opt. Lett.* **27** 2179–81
[25] Binet R, Colineau J and Lehureau J-C 2002 Short-range synthetic aperture imaging at 633 nm by digital holography *Appl. Opt.* **41** 4775–82
[26] Kreiss T and Schlüter K 2007 Resolution enhancement by aperture synthesis in digital holography *Opt. Eng.* **46** 055803
[27] Di J, Zhao J, Jiang H, Zhang P, Fan Q and Sun W 2008 High resolution digital holographic microscopy with a wide field of view based on a synthetic aperture technique and use of linear CCD scanning *Appl. Opt.* **47** 5654–8
[28] Martínez-León L and Javidi B 2008 Synthetic aperture single-exposure on-axis digital holography *Opt. Express* **16** 161–9
[29] Schwarz Ch J, Kuznetsova Y and Brueck S R 2003 Imaging interferometric microscopy *Opt. Lett.* **28** 1424–6
[30] Micó V, Zalevsky Z, García-Martínez P and García J 2006 Superresolved imaging in digital holography by superposition of tilted wavefronts *Appl. Opt.* **45** 822–8
[31] Micó V, Zalevsky Z and García J 2006 Superresolution optical system by common-path interferometry *Opt. Express* **14** 5168–77
[32] Indebetouw G, Tada Y, Rosen J and Brooker G 2007 Scanning holographic microscopy with resolution exceeding the Rayleigh limit of the objective by superposition of off-axis holograms *Appl. Opt.* **46** 993–1000
[33] Kuznetsova Y, Neumann A and Brueck S R J 2007 Imaging interferometric microscopy—approaching the linear system limits of optical resolution *Opt. Express* **15** 6651–63
[34] Price J R, Bingham P R and Thomas C E Jr 2007 Improving resolution in microscopic holography by computationally fusing multiple, oblique illuminated object waves in the Fourier domain *Appl. Opt.* **46** 827–33
[35] Micó V, Zalevsky Z and García J 2008 Common-path phase-shifting digital holographic microscopy: a way to quantitative imaging and superresolution *Opt. Commun.* **281** 4273–81
[36] Micó V, Zalevsky Z, Ferreira C and García J 2008 Superresolution digital holographic microscopy for three-dimensional samples *Opt. Express* **16** 19260–70
[37] Kadono H, Takai N and Asakura T 1987 New common-path phase-shifting interferometer using a polarization technique *Appl. Opt.* **26** 898–904
[38] Mercer C R and Creath K 1994 Liquid-crystal point-diffraction interferometer *Opt. Lett.* **19** 916–8
[39] Medecki H, Tejnil E, Goldberg K A and Bokor J 1996 Phase-shifting point diffraction interferometer *Opt. Lett.* **21** 1526–8
[40] Iemmi C, Moreno A and Campos J 2005 Digital holography with a point diffraction interferometer *Opt. Express* **13** 1885–91
[41] Neal R M and Wyant J C 2006 Polarization phase-shifting point-diffraction interferometer *Appl. Opt.* **45** 3463–76